International Journal of Applied Engineering Research ISSN 0973-4562 Volume 16, Number 6 (2021) pp. 447-458

Wind Turbine Yaw Angle Controller using Artificial Neural Networks Implemented on Embedded System

David Esteban Albadan Molano[1], Diego Alejandro Barragán Vargas[2] and Jorge Enrique Salamanca[3]

[1]*Universidad Distrital Francisco José de Caldas;*

[2]*Universidad Distrital Francisco José de Caldas;*

[3]*Universidad Distrital Francisco José de Caldas;*

Abstract

In this research, artificial neural networks (ANN) developed in python are compared and later compiled in a Raspberry pi 4 to generate a predictive wind direction signal as wind turbine control system input, to maximize the capture of wind power. A set of 12 weather station measured variables are used to feed the neural network, including time, PM10, PM25, and Ozone as secondary variables that will allow enriching the predictive factors of the neural network, the variables NO, NO2, NOX, and SO2, as auxiliary variables that will allow strengthening the validation of the behavior of the network and finally the variables Wind Speed, temperature, relative humidity and wind direction as main variables that will increase the prediction efficiency and with this, to complete partial dependence between the variables is analyzed to improve the ANN convergence time on the embedded system, as future work, it will allow the testing of a control system including control actuators to optimize the network.

Keywords: Wind Turbines, Artificial Neural network controller, Yaw angle, Wind direction

1. INTRODUCTION

Renewable energy is a classification given for the energy produced or obtained by the resources transfer that can be restored naturally at a higher speed than consumed by humans [1]. Wind energy is a good example of the capture, development, and use of renewable natural resources, however, its applications need to receive more attention and research, standing out the fact that in many countries this technology is still very incipient [2]. Nevertheless, it is important to highlight the estimated short-term depletion of fossil fuels, which allows different renewable energies such as wind and solar energy to be promoted in those countries,[3]. Currently, wind energy approaches focus on increasing capture efficiency through wind prediction, given the large number of stochastic variables that allow a correct prediction in the wind turbine's performance, as is the case of wind power, wind speed, power, and direction [4], [5].

Currently, research efforts in wind speed prediction have been made using different mathematical models, metaheuristic, and artificial intelligence models [6-11], finding these last (AI) methods as the more extended and implemented of the recent decades [12], given that AI is the science that facilitates technological systems to emulate human behavior characterized mainly by processes associated with the brain [13], generating enormous advantages in the area of computer electronics power, through allowing the design of integrated and robust systems that can be adapted to real situations, improving significantly autonomy and, indirectly, allows continuous improvement of the system by analyzing multiple architectures through different variables.

In this document, an artificial neural network is implemented in python and tested on a raspberry pi 4 as a control processor device, to control the yaw angle of a wind turbine, considering different related variables such as wind speed and direction, humidity, solar radiation, barometric pressure, and temperature, bearing in mind that the simulated and used data come from a meteorological station. The implemented algorithm is a multilayer backpropagation perceptron that is enhanced through analyzing the different correlations and partial dependence between each variable and the wind direction, to establish their different weight in the behavior of the final prediction of the experiment.

2. SOME CHARACTERISTICS OF THE WIND AND ITS SAMPLE SPACE

The wind is associated with moving air, as a consequence of the uneven heating of the air on the earth's surface and the rotation of the earth, which in turn create global patterns of air circulation in the atmosphere, which vary according to the zone, area and time of year [14]. The wind energy is contained in moving air particles, whose kinetic energy is determined by the following expression:

$$\mathrm{Ke} = \frac{1}{2} \cdot m \cdot v^2 \tag{1}$$

Where m is the air mass and v correspond to the wind speed. Wind by nature is stochastic [15], [16], [17], which means that it changes continuously, statistical models must be generated that describe the different probabilities of the various parameters that it contains immersed in its behavior [18], [19], so it is essential to always visualize the global sample space of the problem and the components of each subset, for this purpose in this document different random variables were taken into accounts such as Time, PM10, Ozone, NO, NO_2, NO_X, SO_2, WindSP (wind speed), Temperature, PM25, RH (relative humidity) and Windir (wind direction). The global sample space is determined by the following equations:

$$\Omega = \{\mathrm{Time}, \mathrm{PM10}, \mathrm{OZONE}, \mathrm{NO}, \mathrm{NO2}, \mathrm{NOX}, \mathrm{SO2}, \mathrm{WindSP}, \mathrm{Temp}, \mathrm{PM2.5}, \mathrm{RH}, \mathrm{WinDir}\} \tag{2}$$

The corresponding power set is:

$$|\boldsymbol{P(s)}| = \boldsymbol{2^{\Omega} = 2^{12} = 4096} \tag{3}$$

The cardinality of the given global sample space is 12, because it has 12 analysis parameters. The three events in the sample space are determined by:

$$\boldsymbol{A} = \{\boldsymbol{Time}, \boldsymbol{PM10}, \boldsymbol{PM2.5}, \boldsymbol{OZONO}\} \tag{4}$$

$$\boldsymbol{B} = \{\boldsymbol{NO}, \boldsymbol{NO2}, \boldsymbol{NOX}, \boldsymbol{SO2}\} \tag{5}$$

$$\boldsymbol{C} = \{\boldsymbol{Temp}, \boldsymbol{RH}, \boldsymbol{WindDir}, \boldsymbol{WindSP}\} \tag{6}$$

Where $A \subset \Omega$, $B \subset \Omega$, and $C \subset \Omega$, event A contains secondary variables that allow reviewing and analyzing key moments in the behavior of a wind turbine throughout the day, given the behavior of different types of microparticles and our atmosphere in general, event B contains auxiliary variables that allow characterizing different concentrations in ppm of various components in the environment and finally, C has the classic variables that are used in the prediction of the behavior of the wind and therefore the wind generator. There exists an event field F, which is a class of subsets of Ω and satisfies the following axioms:

- F is not empty.
- If $A \subset \Omega$ is such that $A \in F$ then $A^C \in F$.
- If A, B and C $\subset \Omega$ are such that A, B, C $\in$ F then A U B U C $\in$ F.

Now, since an artificial neural network will be worked with a database that will have the 12 variables mentioned above for training and validation, it can be observed that each of them manages its own sample space, since its behavior is stochastic, at next, the analysis of each of the different variables is carried out, starting with the table 1 that shows the extreme values that they cover:

Table 1. Extreme parameter values.

Variable	Maximum	Minimum
TIME	1	24
PM10	1.1	251.3
OZONO	3.0	70.6
NO	0	213.4
NO2	-0.5	53
NOX	1.3	243.8
SO2	0.3	9
WIND_SP	0.2	13.4
TEMP	8.3	22.9
PM2.5	0	168.4
RH	27	92
WIN_DIR	0	360

By observing table 1, it is possible to visualize the range and the elements that each sample space in particular covers, the first variable that will be taken into account in the ANN is time, which has 24 daily values that makeup 24 hours a day, as shown below:

$$\boldsymbol{Time} = \{\boldsymbol{1}, \boldsymbol{2}, \dots, \boldsymbol{24}\} \tag{7}$$

The second variable named PM_{10} has 2502 values, because each value is increased 0.1, as shown below:

$$\boldsymbol{PM10} = \{\boldsymbol{1.1}, \boldsymbol{1.2}, \dots, \boldsymbol{251.3}\} \tag{8}$$

The set of powers of this experimental variable is:

$$|\boldsymbol{P(s)}| = \boldsymbol{2^{\Omega} = 2^{2502}} \tag{9}$$

The third variable named OZONO that has 676 values, because each value is increased 0.1, as shown below:

$$\boldsymbol{OZONO} = \{\boldsymbol{3.0}, \boldsymbol{3.1}, \dots, \boldsymbol{70.6}\} \tag{10}$$

The set of powers of this experimental variable is:

$$|\boldsymbol{P(s)}| = \boldsymbol{2^{\Omega} = 2^{676}} \tag{11}$$

The fourth variable named NO that 2135 values, because each value is increased 0.1, as shown below:

$$\boldsymbol{NO} = \{\boldsymbol{0}, \boldsymbol{0.1}, \dots, \boldsymbol{213.4}\} \tag{12}$$

The set of powers of this experimental variable is:

$$|\boldsymbol{P(s)}| = \boldsymbol{2^{\Omega} = 2^{2135}} \tag{13}$$

The fifth named NO2 that 535 values, because each value is increased 0.1, as shown below:

$$\boldsymbol{NO2} = \{\boldsymbol{-0.5}, \boldsymbol{-0.4}, \dots, \boldsymbol{0}, \dots, \boldsymbol{53}\} \tag{14}$$

The set of powers of this experimental variable is:

$$|\boldsymbol{P(s)}| = \boldsymbol{2^{\Omega} = 2^{535}} \tag{15}$$

The sixth variable NOX has 2425 values, each value is increased 0.1, as shown below:

$$\boldsymbol{NOX} = \{\boldsymbol{1.3}, \boldsymbol{1.4}, \dots, \boldsymbol{243.8}\} \tag{16}$$

The set of powers of this experimental variable is:

$$|\boldsymbol{P(s)}| = \boldsymbol{2^{\Omega} = 2^{2425}} \tag{17}$$

The seventh variable named SO2 that 87 values, because each value is increased 0.1, as shown below:

$$\boldsymbol{SO_2} = \{\mathbf{0.3}, \mathbf{0.4}, \ldots, \mathbf{9}\} \tag{18}$$

The set of powers of this experimental variable is:

$$|\boldsymbol{P}(\boldsymbol{s})| = \mathbf{2}^{\boldsymbol{\Omega}} = \mathbf{2}^{\mathbf{87}} \tag{19}$$

The eighth variable is the wind speed named WindSP in the data base and takes 132 values due to each value is increased 0.1, as shown below:

$$\boldsymbol{WindSP} = \{\mathbf{0.2}, \mathbf{0.3}, \ldots, \mathbf{13.4}\} \tag{20}$$

The set of powers of this experimental variable is:

$$|\boldsymbol{P}(\boldsymbol{s})| = \mathbf{2}^{\boldsymbol{\Omega}} = \mathbf{2}^{\mathbf{132}} \tag{21}$$

The ninth variable is the temperature named Temp in the database and has 146 values, each value is increased 0.1, as shown below:

$$\boldsymbol{Temp} = \{\mathbf{8.3}, \mathbf{8.4}, \ldots, \mathbf{22.9}\} \tag{22}$$

The set of powers of this experimental variable is:

$$|\boldsymbol{P}(\boldsymbol{s})| = \mathbf{2}^{\boldsymbol{\Omega}} = \mathbf{2}^{\mathbf{146}} \tag{23}$$

The tenth variable PM2.5 has 1685 values, each value is increased 0.1, as shown below:

$$\boldsymbol{PM}\mathbf{2.5} = \{\mathbf{0}, \mathbf{0.1}, \mathbf{0.2}, \ldots, \mathbf{168.4}\} \tag{24}$$

The set of powers of this experimental variable is:

$$|\boldsymbol{P}(\boldsymbol{s})| = \mathbf{2}^{\boldsymbol{\Omega}} = \mathbf{2}^{\mathbf{12}} \tag{25}$$

The eleventh variable is the relative humidity named RH in the data base, takes 65 values, each value is increased 1, as shown below:

$$\boldsymbol{RH} = \{\mathbf{27}, \mathbf{28}, \mathbf{29}, \ldots \mathbf{92}\} \tag{26}$$

The power set of this experimental variable is:

$$|\boldsymbol{P}(\boldsymbol{s})| = \mathbf{2}^{\boldsymbol{\Omega}} = \mathbf{2}^{\mathbf{65}} \tag{27}$$

The twelfth variable is the wind direction named WinDir in the database is the goal variable which has 361 values, increased each 1 degree, as shown below:

$$\boldsymbol{WinDir} = \{\mathbf{0}, \mathbf{1}, \mathbf{2}, \ldots, \mathbf{360}\} \tag{28}$$

The power set of this experimental variable is:

$$|\boldsymbol{P}(\boldsymbol{s})| = \mathbf{2}^{\boldsymbol{\Omega}} = \mathbf{2}^{\mathbf{361}} \tag{29}$$

3. COMPUTATIONAL METHODS FOR WIND TURBINE CONTROLLING

There are different methods and computational functions that have been developed and implemented in wind turbines to control the yaw angle, an example is a modified climbing control method (HCC) which adopts the different control steps obtained through the algorithm of the bisector plane during search procedure [20], another observed method is the generation of different algorithms based on the vane control and on power detection scaling algorithms that are compiled and run in PLC modules [21]. Other articles comment on the study of methods classics such as maximum power point tracking (MPPT) control for below-rated wind speed operation and yaw and stall control for above-rated wind speed operation [22] [23]. Another important method is yaw angle misalignment and analysis for agile system correction to improve overall performance [24], annexed to the above there are other systems that seek by means of algorithms to always be in a windward mode to take full advantage of the system [25]. Another great branch of analysis and study for the yaw control of a wind turbine is in different forms of optimization, for the maximization of performance [26][27]. There are also different predictive models, which seek to predict the yaw error using different control sets [28][29][30].

Machine learning methods are producing promising results, where different reinforcement algorithms have been developed to control variable speeds with the yaw control [31]. Other methods used are those related to predictive neural algorithms such as those discussed by H Sun et al, in [32], Z. Dzulfikri et al, in [33] Zi Lin et al, in [34], and Bahaghighat et al, in [35].

4. DATA ANALYSIS AND PREPROCESSING

The data used to feed the neural network is a set of 12 variables measured by a meteorological station from 01-10-2020 at 01:00 until 14-01-2021 at 00:00, with a time resolution of 1 hour, for a total of 2519 values per variable and a total of 27709 values to train and validate the neural network architecture. The variables measured by this meteorological station model are:

- Wind direction: Is the goal variable represented by an angle in degrees from 0° to 360°.
- PM10: particles of dust, ash, soot, metallic particles, cement, or pollen, dispersed in the atmosphere, measured in µg/m3 with an aerodynamic diameter less than 10 µm [36][37].
- PM2.5: Small particles suspended in the air with a diameter of less than 2.5 µm, including organic chemicals, dust, soot, and metals. Specifically, coming from all kinds of combustion, such as cars, trucks, factories, wood-burning, agricultural burning, and other activities [38].
- Ozone: Concentration of trioxygen O3 in the atmosphere, usually two to eight parts per million above the surface [39].
- NO, NO2, NOX: nitrogen oxide NO concentration in ppm, further oxidized nitrogen dioxide NO2 and further air pollutant species i.e NOX [40].

International Journal of Applied Engineering Research ISSN 0973-4562 Volume 16, Number 6 (2021) pp. 447-458

- SO2: Level of sulfur dioxide in the atmosphere measured in ppb which seems to be closely related with the wind [41, 42, 43].
- Ambient temperature: Gives the temperature in °C from 0 °C to 50°C, at a height of 15 meters.
- Relative Humidity: Gives the relative humidity in a range from 20% to 90%.
- Wind speed: Gives the wind speed at a height of 22 meters.
- Time: gives the time in with the measure is taken.

Some researchers have discussed the relation between different kinds of particles and molecules in the air and certain meteorological features related to the wind speed and direction [44, 45, 46, 47, 48, 49], therefore, it has been taken into account every variable measured by the weather station including those that do not have an obvious relation with the wind parameters. Additionally, will be carried out a partial dependence analysis to establish the actual impact of each variable.

The weather station is located at 4°40'12.36"N, 74°8'29.58"W, at an altitude of 2591 m above sea level and 15 m above the ground for the sensors except for the anemometer which is 22 m above the ground. Using the pandas function describe() in python have been generated descriptive statistics of the data including percentiles 25, 50, and 75, dispersion and shape of a dataset's distribution, without taking into account NaN values [50], the results are shown in Table 2, where the statistical data is, Min: minimum value, Max: that is the maximum value, Mean is the variable average value and STD corresponds to the standard deviation.

The box plots of the wind direction, wind speed, relative humidity, and temperature are shown in figure 1, these plots with the histograms shown in figure 2, have been useful to identify the distribution of the values in the variable which will be taken into account when designing the control system.

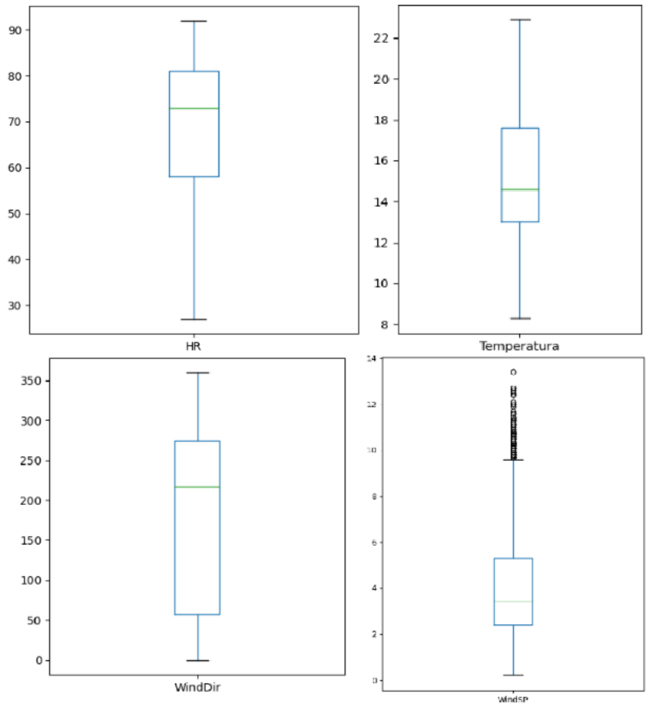

Figure 1. Box plot diagram for relative Humidity, Temperature, Wind direction and wind speed.

Table 2. Data statistical description.

Summary	Time	PM10	PM25	Ozone	NO	NO2	NOX	WindSp	Temp	HR	Wind Dir	SO2
Count	2519	2519	2519	2519	2519	2519	2519	2519	2519	2519	2519	2519
Mean	12.5	34.3	19.1	17.9	13.5	16.5	30.0	4.1	15.1	68.6	182.4	1.2
Std	6.9	21.8	11.5	12.6	19.4	8.6	25.1	2.3	2.8	14.7	114.4	0.8
Min	1.0	1.1	0.0	3.0	0.0	0.5	1.3	0.2	8.3	27.0	0.0	0.3
25%	6.5	19.5	11.3	6.5	2.6	9.9	13.4	2.4	13.0	58.0	57.5	0.8
50%	12.0	29.6	17.0	15.2	5.7	19.4	22.4	3.4	14.6	73.0	218.0	0.9
75%	18.5	43.3	24.3	26.9	15.9	22.3	38.5	5.3	17.6	81.0	270.0	1.3
Max	24.0	251.3	198.4	70.6	213.4	53.0	243.8	13.4	22.9	92.0	360.0	9.0

[1] Meteorological station data statistics.

The variables have been labeled so: WindDir is the wind direction in degrees, Temperatura that is the temperature in °C, HR is the relative humidity and WindSP is the wind speed measured in meters per second; Notice that the wind direction training data cover a range from 0° to 360°, therefore the training data cover the entire range of the dynamic system; this fact increases the accuracy of the algorithm.

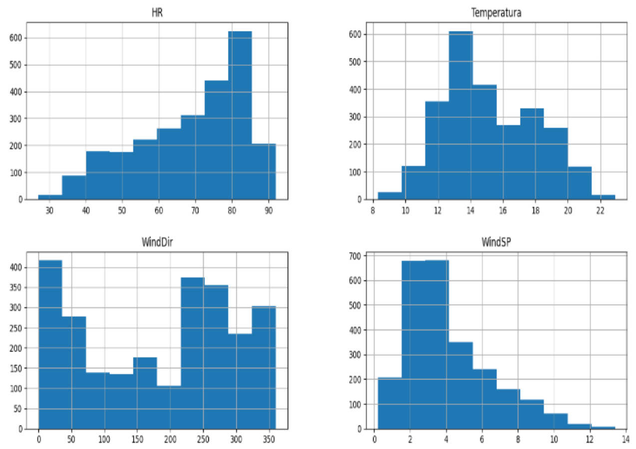

Figure 2. Data histograms.

It turns out from figure 2 that the variables: relative humidity, temperature, and wind speed follow quasi-normal distributions but the goal variable (Wind direction) does not have a normal distribution of probability, instead seem to be the most randomly distributed one, that is the main reason why its most appropriate to implement a non-linear control system like a neural network-based one; the figure 2 has been obtained using the matplotlib function hist() in python, which has integrated the required code to plot histograms in a python environment [51].

To accomplish the main goals of a wind turbine controller, which are: extract the maximum power of the wind, good electrical connection to the network and avoid physical damages [52], the majority of commercial wind turbines implement: voltage pulse width modulation (PWM) controllers, maximum power point tracking (MPPT) techniques and pitch angle controllers [53, 54], neither of these controllers stand the wind direction which is by far the most random variable find in this research, this is another reason to design and implement better controllers than the traditional ones.

The last analysis carried out with the data is the multivariate analysis, in doing so, scatter plots have been obtained to find some patterns and relations between the variables, displaying the data as coordinate points where the x-position of the point is determined by one variable and the y-position is determined by the other one, both measured at the same time [55], the figure 3 shows the scatter plots of the variables in which occurs three different kinds of relations between variables:

- Positive correlation: occurs when the slope of the correlation is positive [56], it is observed clearly in the variables NOx with NO, and PM10 with PM2.5, and in a more diffuse way NO2 with NOX, NO2 with NO, and temperature with ozone.
- A negative correlation occurs when the slope of the correlation is negative [56], it observed in the variables temperature and relative humidity (HR).
- No correlations: occurs when there is no appreciable relationship between the variables [57], is important to note that this relation regards mainly to high dispersion of the points over the scatter plot, not too complex or non-linear relations that could be linearized to obtain useful information.

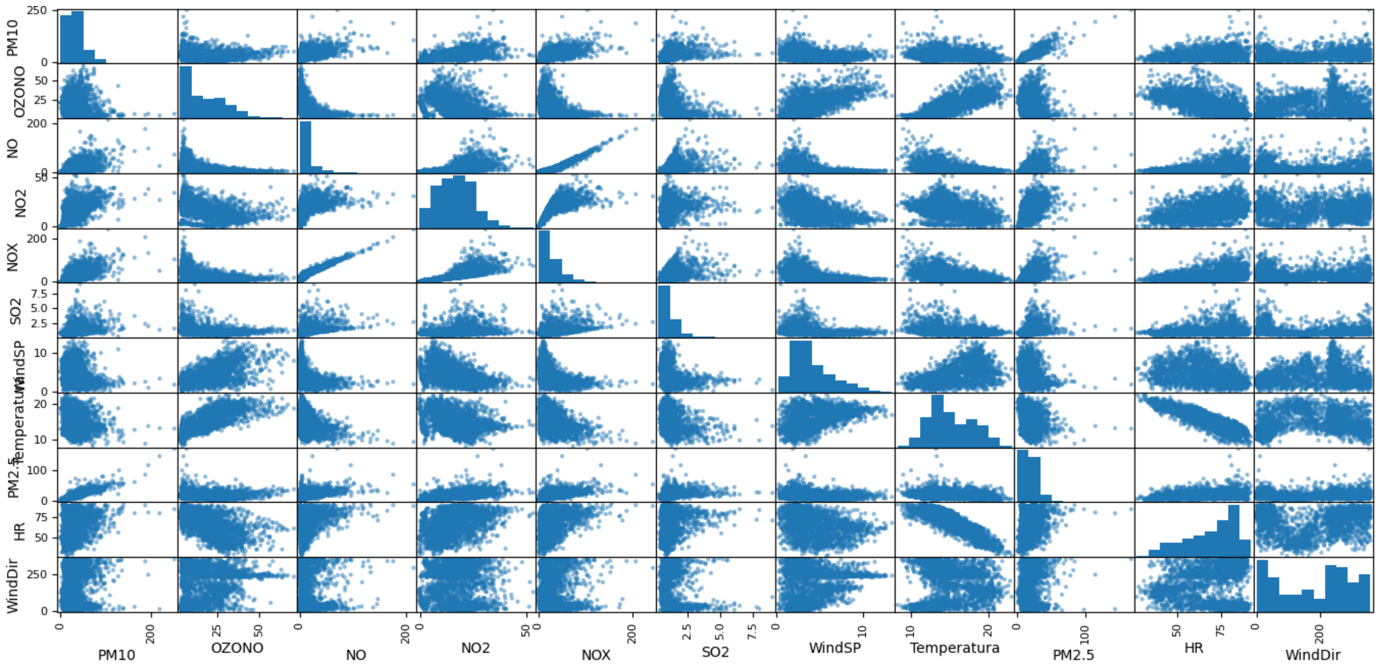

Figure 3. Scatter plot of the variables.

The scatter plot analysis would allow us to conclude that under linear combinations the variables NOx with NO, and PM10 with PM2.5, could be combined to reduce the number of inputs to the ANN and in doing so reducing the computational load of the neural network, which will be especially useful when implementing the architecture on an embedded system like Raspberry Pi 4, this combination would be performed only if the partial dependence analysis, developed in the next section, validates the utility of doing so and this hypothesis will be subject to validation under the verification of the correlation coefficient before and after modifying the ANN number of the inputs.

5. PARTIAL DEPENDENCE ANALYSIS

The ability of neural networks to discover hidden and complex patterns in the data has exceeded human capacity [58, 59, 60, 61] therefore to understand these patterns and associated relation between variables its important to use simplification tools [62, 63], in this section is implemented the partial dependence analysis which consists in solving the equation 30, to find the marginal dependence between the goal variable and a certain related variable [64, 65], in this work the partial dependence analysis will be carried out between the goal variable and maximum 2 features due to the results for 3 or even more features results extremely complex to analyze.

$$\widehat{\boldsymbol{g}}_{\boldsymbol{xs}}(\boldsymbol{x}_{\boldsymbol{s}}) = \boldsymbol{E}_{\boldsymbol{x}_{\boldsymbol{c}}}\left[\widehat{\boldsymbol{g}}_{\boldsymbol{x}_{\boldsymbol{s}}}(\boldsymbol{x}_{\boldsymbol{s}}, \boldsymbol{x}_{\boldsymbol{c}})\right] = \int \widehat{\boldsymbol{g}}_{\boldsymbol{x}_{\boldsymbol{s}}}(\boldsymbol{x}_{\boldsymbol{s}}, \boldsymbol{x}_{\boldsymbol{c}})\boldsymbol{dP}(\boldsymbol{x}_{\boldsymbol{c}}) \tag{30}$$

Where $\widehat{\boldsymbol{g}}_{\boldsymbol{xs}}$ is the neural network model $\boldsymbol{x}_{\boldsymbol{s}}$ corresponds to the feature vector or related variable which will be composed of a maximum of 2 features and $\boldsymbol{x}_{\boldsymbol{c}}$ is the goal variable or prediction. This analysis has remarkable importance to find those features which perform an appreciable impact in the goal variable [66] which are worth including in the neural network model that will be implemented in the Raspberry Pi 4, for the sake of avoiding unnecessary computational load, the features founded to have a close relationship between them are also analyzed in a 2-d partial dependence to corroborate if a linear combination is viable, to reduce even more the computational load.

To compute the partial dependence is necessary to implement a black box model [67], in this work the model is a neural network $\widehat{\boldsymbol{g}}_{\boldsymbol{xs}}$ that is trained first in a computer until it reaches reasonable results regarding the coefficient of determination and the computation time, in the next section is implemented the architecture on a Raspberry Pi 4 with the corresponding adjustment to decrease the computational load. The neural network architecture is shown in table 3, notice that this network has not been subjected to all rigorous validation processes due to this architecture is only developed to obtain the partial dependence relationships and as a basis for the final architecture implemented in the embedded system, fine-tuning will be carried out in said implementation.

Table 3. Initial ANN parameters.

Parameter	**Configuration**
Activation function	tanh
Optimizer	ADAM
Training data	80%
Validation data	20%
R^2	0.99855
Architecture	[12, 10, 1]
learning rate (init)	0.4
Time	0.23 s

Table 3 shows the parameters and the respective configurations used in the artificial neural networks, for example, in the activation function, the hyperbolic tangent function was used, which allows an evaluation interval of [-1,1] giving a good margin of analysis to observe the change of the different data. The optimizer used for the training of the artificial neural network was ADAM since it allows the learning rate of each iteration to have a range after the correction made to each displacement so that the parameters are relatively stable [93, 94, 95]. Then the fractionation of the database is shown in table III, where 80% was used to train the network and 20% was used for the validation of the behavior of each architecture. To finally detail the correlation, architecture, learning rate, and time obtained.

To compute the ANN has been used the sklearn library in python, specifically is used the neural network regressor model: MLPRegressor [68], using the fact that the ANN regressor has the characteristic to change the domain of the phenomena from a reasonable problem to an algebraically predictable problem [69, 70, 71], in which the goal is to predict the wind direction, using the great ability of ANN to predict stochastic or non-linear relationships [72], as the wind direction. To compute the partial dependence of equation 30 is used the library sklearn. inspection [73] in python, with the command plot_partial_dependence(g_xs, X, features) is also plotted the results shown in Figures 4, 5, and 6.

International Journal of Applied Engineering Research ISSN 0973-4562 Volume 16, Number 6 (2021) pp. 447-458

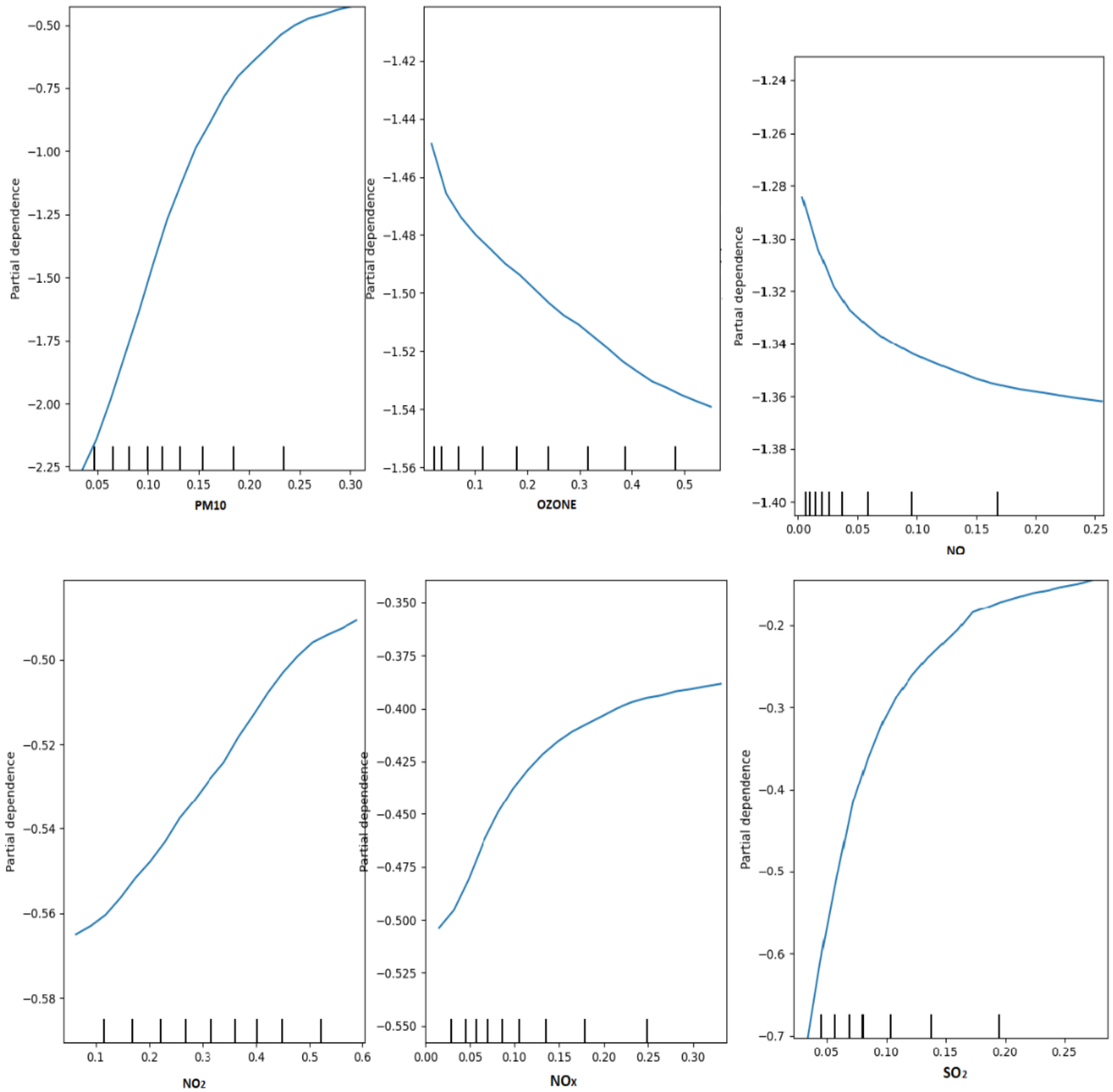

Figure 4. Partial dependence of: PM10, ozone, NO2, NOX, NO and SO_2 respect to wind direction.

In figure 4 is observed that although there is a markedly decreasing relationship between the ozone and the wind direction, the ozone has no noticeable impact due to the tiny numerically change in the y axis, this phenomenon also occurs with the NO2 and NOX but to a lesser extent, NO presents a similar behavior as the ozone concerning the wind direction having a decreasing relation but not an appreciable impact, the variable SO2 presents an appreciable impact in the goal variable that could be easy linearized by algebraic tools [74] e.g logarithmic and potential linearizers or some more sophisticated as shown in [75, 76, 77].

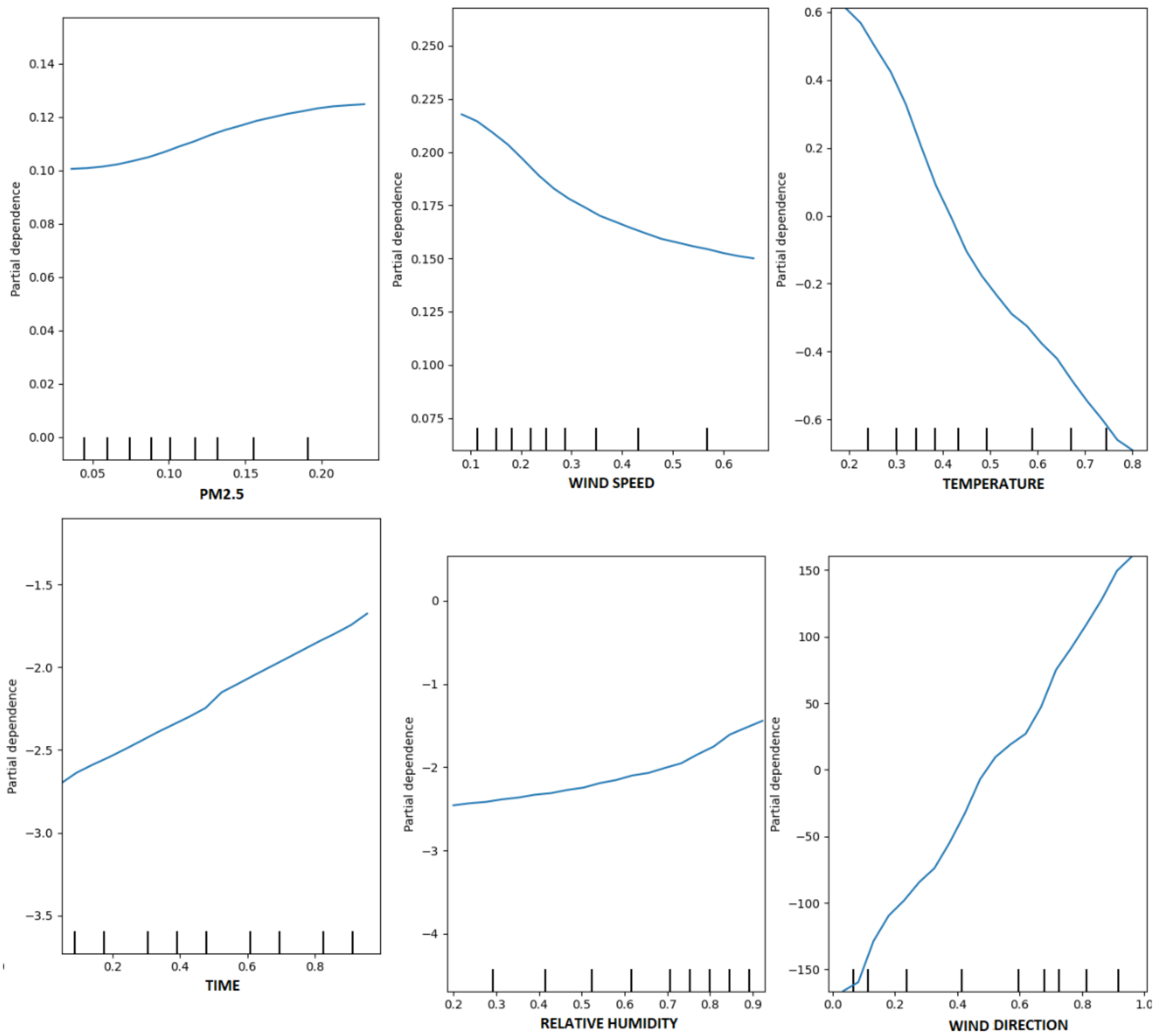

Figure 5. Partial dependence of: PM2.5, Time, Wind speed, relative humidity, and temperature respect to wind direction.

In figure 5 is observed that PM2.5 surprisingly has a small impact concerning wind direction contrary to PM10 despite being closely related, the time represents the hour of the day, the partial dependency analysis has yielded a very interesting result because it shows a not very strong but appreciable linear relationship between the hour of the day and the wind direction; the relationship between the wind speed and the wind direction is not so interdependent as expected where the wind speed seems not to represent an appreciable impact with the wind direction, the temperature presents an appreciable inverse dependence with the wind direction, on the contrary, humidity does not have such a significant impact although it is not so small as to be negligible. As expected the wind directions have a huge interdependence with itself, furthermore, taking into account that the wind direction stands in a normalized range for the partial dependence plots, then each feature is computed with the equation 30 to finally compute the mean values of the output, the results obtained with this process will be valid if and only if the goal feature has not a strong dependence with other feature except itself [78], as shown in figures 4 and 5 any variable has a so deep partial dependence as the wind direction with itself, this result allows to validate that the partial dependence model developed work properly.

Figure 6 is shown the result of the neural network used to obtain the partial dependence in the Linux-Debian environment, these results will be compared with the adjusted neural network once the low impact variables have been eliminated.

```
david@debian:~/Documentos$ python3 nntrain.py
Training MLPRegressor...
Computing time 0.230s
 R2 result: 0.998551
```

Figure 6. Preliminary ANN results.

With the information explained in this section the following adjustments are possible: the ozone will not be taken into account due to its low impact in the goal variable, due to the similar behavior between NOX and NO_2, will be held in the ANN only the one with the higher impact between the two, which is NOX; NO and PM2.5 also present a tiny impact, therefore, these will be taken into account, the time as an input parameter despite not having an appreciable numerical impact will be taken into account for its impressive linear dependence with the wind direction; the SO_2 has an appreciable effect in the goal feature, therefore, will be taken into account.

As the wind speed is the main variable for the power generation in a wind turbine and therefore an important resource for the control system, it will not be eliminated as an input variable to the control system, the temperature has an important partial dependence with the wind direction and also will remain in the final architecture of the ANN, the relative humidity has not enough appreciable impact thus will not be taken into account. With the previous analysis the ANN is newly trained and the result shown in figure 7 is obtained.

```
david@debian:~/Documentos$ python3 nntrain.py
Training MLPRegressor...
Computing time 0.171s
 R2 result: 0.999307
```

Figure 7. Enhanced ANN results.

The comparative analysis between the preliminary ANN and the enhanced ANN is summarized in table 4.

Table 4. Comparative results.

Parameter	Configuration
Time reduction	25.65 %
R^2 increment	0.076 %

Table 4 shows that, contrary to what would be expected, there was not only a decrease in computation time and also an increase in R2, this is mainly because by decreasing the computational load, the number of possible iterations performed by the algorithm increases until reaching the convergence goal. By avoiding including the ozone, NO, NO2, PM2.5, and relative humidity the ANN changes from having 12 input features to 7 inputs which allow avoiding the acquisition of the corresponding sensors and their associated cost, as well as, the number of peripherals destined to the data collection in the Raspberry or in case of being multiplexed, it would improve the sampling rate assigned to each sensor.

6. CONCLUSIONS

ANN are an effective technique to control the YAW angle of wind turbines reaching high accuracy and low computational time. This paper implements an enhanced ANN on a Raspberry pi 4 as the processor module of a control system introducing subjects related to the data measurement, variables correlation, control strategy, between others.

A decreasing relationship was observed between the ozone parameter and the wind speed variable, in figure 4 it is observed that ozone does not have a significant impact due to the minimal numerical change in the y-axis, this appreciation was also observed with the NO2 variable and NOX although in a lesser way. The greatest partial dependence observed was in the variable PM10, also visualized in figure 4.

The best architecture obtained with the activation function tanh and ADAM optimizer was an architecture of 10 hidden neurons as shown in table 3.

REFERENCES

[1] O. Irimia, C. Tomozei, M. Panainte-Lehadus and M. C. Dinu, "Evaluation of the potential of wind energy as a source of electricity generation: Case study - Vanatori Wind Power Plant," 2020 7th International Conference on Energy Efficiency and Agricultural Engineering (EE&AE), Ruse, Bulgaria, 2020, pp. 1-4, doi: 10.1109/EEAE49144.2020.9278983.

[2] A. Kumar, P. B. Karandikar and D. S. Chavan, "Generating and saving energy by installing wind turbines along the railway tracks," 2015 International Conference on Energy Systems and Applications, Pune, India, 2015, pp. 25-27, doi: 10.1109/ICESA.2015.7503307.

[3] Aitor Saenz Aguirre, Ekaitz Zulueta, Unai Fernandez Gamiz, Javier Lozano, Jose Manuel Lopez Guede. "Artificial Neuronal Network-Based Reinforcement Learning for wind turbine yaw control". Rev energies, 2019. 12(3), 436; https://doi.org/10.3390/en12030436.Author 1, A.B.; Author 2, C.D. Title of the article. *Abbreviated Journal Name* **Year**, *Volume*, page range.

[4] D. E. A. Molano and D. A. B. Vargas, "Wind Turbine Yaw Angle Control using Artificial Neural Networks : *Real data is used to feed the neural network," 2020 10th International Conference on Advanced Computer Information Technologies (ACIT), Deggendorf, Germany, 2020, pp. 374-379, doi: 10.1109/ACIT49673.2020.9208855.

[5] Z. Jianli, W. Jiguang, B. Geping and L. Yingjun, "Wind Power Forecasting by Using Artificial Neural Networks and Grubbs Criterion," 2019 22nd International Conference on Electrical Machines and Systems (ICEMS), Harbin, China, 2019, pp. 1-5, doi: 10.1109/ICEMS.2019.8922023.

[6] Jinkyoo Park, Kincho H. Law, Cooperative wind turbine control for maximizing wind farm power using sequential convex programming, Energy Conversion and Management, Volume 101, 2015, Pages 295-316, ISSN 0196-8904, https://doi.org/10.1016/j.enconman.2015.05.031.

[7] W. Xin, L. Yanping and T. Wei, "Modified hill climbing method for active yaw control in wind turbine,"

Proceedings of the 31st Chinese Control Conference, Hefei, China, 2012, pp. 6677-6680.

[8] N. Hure, R. Turnar, M. Vašak and G. Benčić, "Optimal wind turbine yaw control supported with very short-term wind predictions," 2015 IEEE International Conference on Industrial Technology (ICIT), Seville, Spain, 2015, pp. 385-391, doi: 10.1109/ICIT.2015.7125129.

[9] D. VASILIU, N. VASILIU and C. CĂLINOIU, "Dynamics of the Electrohydraulic Yaw Control Systems for Wind Turbines," 2019 International Conference on ENERGY and ENVIRONMENT (CIEM), Timisoara, Romania, 2019, pp. 308-312, doi: 10.1109/CIEM46456.2019.8937664.

[10] Fernandez-Gauna, B.; Fernandez-Gamiz, U.; Grana, M. Variable speed wind turbine controller adaptation by reinforcement learning.Integr. Comput. Aided Eng. 2017, 24, 27–39.

[11] A. Alarabi and M. El-Hawary, "Multidimensional Optimal Control of wind Turbine Generator," 2014 IEEE Electrical Power and Energy Conference, Calgary, AB, Canada, 2014, pp. 104-109, doi: 10.1109/EPEC.2014.37.

[12] S. Zhao, F. Blaabjerg and H. Wang, "An Overview of Artificial Intelligence Applications for Power Electronics," in IEEE Transactions on Power Electronics, vol. 36, no. 4, pp. 4633-4658, April 2021, doi: 10.1109/TPEL.2020.3024914.

[13] [Ricardo Alirio Gonzalez, Roberto Escobar Ferro, Daríoo Liberona, Government and governance in intelligent cities, smart transportation study case in Bogotá Colombia, Ain Shams Engineering Journal, Volume 11, Issue 1, 2020, Pages 25-34, ISSN 2090-4479, https://doi.org/10.1016/j.asej.2019.05.002.

[14] [14] Danitza M. Corte P., Fabio Sierra V, Guillermo E. Valencia O., Mathematical model validation “Probability Density Function (PDF) of Weibull” assessing the wind resource in colombian Caribbean area: case study”, Prospect, Vol 13, N°2, 38-46,2015.

[15] Gevorkyan, M. N., “Approaches to Stochastic Modeling of Wind Turbines”, arXiv:1711.03589, 2017.

[16] Aksoy, Hafzullah & Toprak, Z. & Aytek, Ali & Erdem, N. (2004). Stochastic generation of hourly mean wind speed data. Renewable Energy. 29. 2111-2131. 10.1016/j.renene.2004.03.011.

[17] Angeliki Loukatou, Sydney Howell, Paul Johnson, Peter Duck, Stochastic wind speed modelling for estimation of expected wind power output, Applied Energy, Volume 228, 2018, Pages 1328-1340, ISSN 0306-2619, https://doi.org/10.1016/j.apenergy.2018.06.117.

[18] Vladislovas Katinas, Giedrius Gecevicius, Mantas Marciukaitis, An investigation of wind power density distribution at location with low and high wind speeds using statistical model, Applied Energy, Volume 218, 2018, Pages 442-451, ISSN 0306-2619, https://doi.org/10.1016/j.apenergy.2018.02.163.

[19] Piotr Wais, Two and three-parameter Weibull distribution in available wind power analysis, Renewable Energy, Volume 103, 2017, Pages 15-29, ISSN 0960-1481, https://doi.org/10.1016/j.renene.2016.10.041.

[20] W. Xin, L. Yanping and T. Wei, "Modified hill climbing method for active yaw control in wind turbine," Proceedings of the 31st Chinese Control Conference, Hefei, China, 2012, pp. 6677-6680.

[21] F. Guo, W. Jiang, H. Shao, Y. Du and J. She, "Research on the wind turbine yaw system based on PLC," 2017 29th Chinese Control and Decision Conference (CCDC), Chongqing, China, 2017, pp. 5164-5168, doi: 10.1109/CCDC.2017.7979412.

[22] E. Mohammadi, R. Fadaeinedjad, H. Shariatpanah and G. Moschopoulos, "Performance evaluation of yaw and stall control for small-scale variable speed wind turbines," 2017 IEEE 30th Canadian Conference on Electrical and Computer Engineering (CCECE), Windsor, ON, Canada, 2017, pp. 1-4, doi: 10.1109/CCECE.2017.7946599.

[23] W. Cui, X. Liu, F. Yu and J. Whitty, "Analysis of the passive yaw mechanism of small horizontal-axis wind turbines," 2009 World Non-Grid-Connected Wind Power and Energy Conference, Nanjing, China, 2009, pp. 1-5, doi: 10.1109/WNWEC.2009.5335837.

[24] Y. Bao, Q. Yang, S. Li, K. Miao and Y. Sun, "A data-driven approach for identification and compensation of wind turbine inherent yaw misalignment," 2018 33rd Youth Academic Annual Conference of Chinese Association of Automation (YAC), Nanjing, 2018, pp. 961-966, doi: 10.1109/YAC.2018.8406510.

[25] F. Bu, W. Huang, Y. Hu, Y. Xu, K. Shi and Q. Wang, "Study and implementation of a control algorithm for wind turbine yaw control system," 2009 World Non-Grid-Connected Wind Power and Energy Conference, Nanjing, China, 2009, pp. 1-5, doi: 10.1109/WNWEC.2009.5335830.

[26] N. Hure, R. Turnar, M. Vašak and G. Benčić, "Optimal wind turbine yaw control supported with very short-term wind predictions," 2015 IEEE International Conference on Industrial Technology (ICIT), Seville, Spain, 2015, pp. 385-391, doi: 10.1109/ICIT.2015.7125129.

[27] H. Choi, J. Kim, J. Cho and Y. Nam, "Active yaw control of MW class wind turbine," ICCAS 2010, Gyeonggi-do, Korea (South), 2010, pp. 1075-1078, doi: 10.1109/ICCAS.2010.5669699.

[28] D. R. Song et al., "Model Predictive Control Using Multi-Step Prediction Model for Electrical Yaw System of Horizontal-Axis Wind Turbines," in IEEE Transactions on Sustainable Energy, vol. 10, no. 4, pp. 2084-2093, Oct. 2019, doi: 10.1109/TSTE.2018.2878624.

[29] Tinghui Ouyang, Andrew Kusiak, Yusen He, Predictive model of yaw error in a wind turbine, Energy, Volume 123, 2017, Pages 119-130, ISSN 0360-5442, https://doi.org/10.1016/j.energy.2017.01.150.

[30] Astolfi, Davide; Castellani, Francesco; Natili, Francesco. 2019. "Wind Turbine Yaw Control Optimization and Its Impact on Performance" Machines 7, no. 2: 41. https://doi.org/10.3390/machines7020041

[31] Saenz-Aguirre, Aitor; Zulueta, Ekaitz; Fernandez-Gamiz, Unai; Lozano, Javier; Lopez-Guede, Jose M. 2019.

"Artificial Neural Network Based Reinforcement Learning for Wind Turbine Yaw Control" Energies 12, no. 3: 436. https://doi.org/10.3390/en12030436

[32] Haiying Sun, Changyu Qiu, Lin Lu, Xiaoxia Gao, Jian Chen, Hongxing Yang, Wind turbine power modelling and optimization using artificial neural network with wind field experimental data, Applied Energy, Volume 280, 2020, 115880, ISSN 0306-2619, https://doi.org/10.1016/j.apenergy.2020.115880.

[33] Z. Dzulfikri, ST. Nuryanti, Y. Erdani, Design and Implementation of Artificial Neural Networks to Predict Wind Directions on Controlling Yaw of Wind Turbine Prototype, Journal of Robotics and Control, Volume I, Issue I, 2020.

[34] Zi Lin, Xiaolei Liu, Wind power forecasting of an offshore wind turbine based on high-frequency SCADA data and deep learning neural network, Energy, Volume 201, 2020, 117693, ISSN 0360-5442, https://doi.org/10.1016/j.energy.2020.117693.

[35] Bahaghighat, Mahdi; Xin, Qin; Motamedi, Seyed A.; Zanjireh, Morteza M.; Vacavant, Antoine. 2020. "Estimation of Wind Turbine Angular Velocity Remotely Found on Video Mining and Convolutional Neural Network" Appl. Sci. 10, no. 10: 3544. https://doi.org/10.3390/app10103544

[36] California Environmental Protection Agency. Air Resources Board, ed. (26-09-2011)., Particulate Matter Program, Archived Juni 2012.

[37] Kassomenos,P.A., Vardoulakis,S., Chaloulakou,A., Paschalidou,A.K., Grivas,G., Borge,R., Lumbreras J. (2014) Study of PM10 and PM2.5 levels in three European cities: Analysis of intra and inter urban variations. Atmospheric Environment 87, pp. 153-163.

[38] US EPA, OAR (19 April 2016). "Particulate Matter (PM) Basics". US EPA. Retrieved 11 March 2021.

[39] Hultman, G. Eric (1980-01-01). “The Ozone Survival Manual”. McGraw-Hill. ISBN 9780915498734.

[40] Air Quality Criteria for Ozone and Related Photochemical Oxidants Volume III of III, US Environmental Protection Agency, 2019 (EPA Report)

[41] Ilić, Predrag & Markic, Dragana & Stojanović, Ljiljana. (2018). Variation concentration of sulfur dioxide and correlation with meteorological parameters. Archives for Technical Sciences. 18. 81-88. 10.7251/afts.2018.1018.081I.

[42] Preradović, L., Ilić, P., Marković, S., & Janjuš, Z. (2011). Meteorological parameters and pollution caused by Sulfur dioxide and their influence on construction materials and heritage.Facta universitatis-series: Electronics and Energetics,24(1), pp. 9-20.

[43] Vidaković, M., Djurić, N., Savković, P., & Babić, R. (2013). pH of precipitation in the area of the town of Bijeljina.Archives of Technical SciencesNo 8 (1), pp. 75-80.

[44] [Ilić, Predrag. (2009). Quality control and research of air pollution influence in function of protection and environmental improvement in Banja Luka. Doctor thesis, University of Novi Sad. 12/2009

[45] Galindo,N., Varea,M., Gil-Molto,J., Yubero,E., Nicolas,J. (2011). Influence of meteorology on particulate matter concentrations at an urban Mediterranean location. Water Air Soil Pollution 215, pp. 365-372.

[46] Krynicka,J., Drzeniecka-Osiadacz,A. (2013). Analysis of variability in PM10 concentration in the Wroclaw agglomeration. Polish journal of environmental studies 22, pp. 1091-109

[47] Li L., Qian,J., Ou C-Q., Zhou,Y-X, Guo,C., Guo,Y. (2014). Spatial and temporal analysis of Air Pollution Index and its time scale-dependet relationship with meteorological factors in Guangzhou, China, 2001-2011, Environmental Pollution 190, pp. 75-81.

[48] Lin,M., Tao,J., Chan,C-Y, Cao J-J., Zhang,Z-S., Zhu,L-H, Zhang,R-J., (2012).Regression analyses between air quality and visibility changes in megacities at four haze regions in China. Aerosol and air quality research 12, pp. 1049-1061.

[49] Zhang,H., Wang Y., Hu,J., Ying,Q, Hu, X-M, (2012). Relationships between meteorological parameters and criteria air pollution in three megacities in China. Environmental Research 140, pp. 242-254

[50] pandas.DataFrame.describe.(2021). Pydata. Accessed: March. 11, 2021. [Online]. Available: https://pandas.pydata.org/docs/reference/api/pandas.DataFrame.describe.html

[51] S. Singh. “Matplotlib.pyplot.hist() in Python”, www.geeksforgeeks.org, https://auth.geeksforgeeks.org/user/SHUBHAMSINGH10/profile (Acessed on 15. March 2021)

[52] D. Eltigani, S. Masri, Challenges of integrating renewable energy sources to smart grids: a review. Renew. Sustain. Energy Rev., 52 (2015), pp. 770-780

[53] R. Tiwari, N.R. BabuRecent developments of control strategies for wind energy conversion system Renew. Sustain. Energy Rev., 66 (2016), pp. 268-285

[54] E.J.N. Menezes, A.M. Araújo, da Silva, Nadège Sophie Bouchonneau A review on wind turbine control and its associated methods J. Clean. Prod., 174 (2018), pp. 945-953.

[55] Utts, Jessica M. Seeing Through Statistics 3rd Edition, Thomson Brooks/Cole, 2005, pp 166-167. ISBN 0-534-39402-7

[56] Emerson, John W.; Green, Walton A.; Schoerke, Barret; Crowley, Jason (2013). "The Generalized Pairs Plot". Journal of Computational and Graphical Statistics. 22 (1): 79–91. doi:10.1080/10618600.2012.694762.

[57] Zador, A.M. A critique of pure learning and what artificial neural networks can learn from animal brains. Nat Commun 10, 3770 (2019). https://doi.org/10.1038/s41467-019-11786-6

[58] Hassabis, D., Kumaran, D., Summerfield, C. & Botvinick, M. Neuroscience-inspired artificial intelligence. Neuron 95, 245–258 (2017).

[59] Antolet, S. et al. Vqa: Visual question answering. In Proceedings of the IEEE International Conference on Computer Vision, 2425– 2433 (2015).

[60] Silver, D. et al. A general reinforcement learning algorithm that masters chess, shogi, and go through self-play. Science 362, 1140–1144 (2018).

[61] Kohoutová, L., Heo, J., Cha, S. et al. Toward a unified framework for interpreting machine-learning models in neuroimaging. Nat Protoc 15, 1399–1435 (2020). https://doi.org/10.1038/s41596-019-0289-5

[62] Fan, Q., Zhou, G., Gui, T. et al. Advancing theoretical understanding and practical performance of signal processing for nonlinear optical communications through machine learning. Nat Commun 11, 3694 (2020). https://doi.org/10.1038/s41467-020-17516-7

[63] L. Wang, X. Tang, J. Zhang and D. Guan, "Correlation Analysis for Exploring Multivariate Data Sets," in IEEE Access, vol. 6, pp. 44235-44243, 2018, doi: 10.1109/ACCESS.2018.2864685.

[64] Zhao, Qingyuan, and Trevor Hastie. "Causal interpretations of black-box models." Journal of Business & Economic Statistics, to appear. (2017)

[65] Friedman, Jerome H. "Greedy function approximation: A gradient boosting machine." Annals of statistics (2001): 1189-1232.

[66] Apley, Dan. 2018. ALEPlot: Accumulated Local Effects (Ale) Plots and Partial Dependence (Pd) Plots. https://CRAN.R-project.org/package=ALEPlot.

[67] Greenwell, Brandon M. 2017. "Pdp: An R Package for Constructing Partial Dependence Plots." The R Journal 9 (1): 421–36. https://journal.r-project.org/archive/2017/RJ-2017-016/index.html.

[68] Pedregosa, F., Varoquaux, G., Gramfort, A., Michel, V., Thirion, B., Grisel, O., Blondel, M., Prettenhofer, P., Weiss, R., Dubourg, V., Vanderplas, J., Passos, D., Brucher, M., Perrot, M., & Duchesnay, E. (2011). Scikit-learn: Machine Learning in Python. Journal of Machine Learning Research, 12, 2825–2830.

[69] Rahman, N. H. A., Lee, M. H., Suhartono & Latif, M. T. Artificial neural networks and fuzzy time series forecasting: An application to air quality. Qual. Quant. 49, 1–15 (2015). Return to ref 21 in article

[70] Kyriakidis, I., Karatzas, K., Kukkonen, J., Papadourakis, G. & Ware, A. Evaluation and analysis of artificial neural networks and decision trees in forecasting of common air quality index in Thessaloniki, Greece. Eng. Intell. Syst. Electr. 2, 111–124 (2013).

[71] Tu, J. V. Advantages and disadvantages of using artificial neural networks versus logistic regression for predicting medical outcomes. J. Clin. Epidemiol. 49, 1225–1231 (1996).

[72] Liu, B., Zhao, Q., Jin, Y. et al. Application of combined model of stepwise regression analysis and artificial neural network in data calibration of miniature air quality detector. Sci Rep 11, 3247 (2021). https://doi.org/10.1038/s41598-021-82871-4

[73] sklearn.inspection.(2020). scikit-learn 0.24.1. Accessed: March. 12, 2021. [Online]. Available: https://scikit-learn.org/stable/modules/classes.html#module-sklearn.inspection

[74] Leonov, G. A.; Kuznetsov, N. V. (2007). "Time-Varying Linearization and the Perron effects". International Journal of Bifurcation and Chaos. 17 (4): 1079–1107. https://doi.org/10.1142/S0218127407017732.

[75] Fletcher, A., Macclure, D. On Quasiregular Linearizers. Comput. Methods Funct. Theory 15, 263–276 (2015). https://doi.org/10.1007/s40315-014-0100-0

[76] Fletcher, A., Macclure, D. Strongly automorphic mappings and Julia sets of uniformly quasiregular mappings. JAMA 141, 483–520 (2020). https://doi.org/10.1007/s11854-020-0107-6

[77] J.F. Groote, A. Ponse, Y.S. Usenko, Linearization in parallel pCRL, The Journal of Logic and Algebraic Programming, Volume 48, Issues 1–2, 2001, Pages 39-70, ISSN 1567-8326, https://doi.org/10.1016/S1567-8326(01)00005-4.

[78] A. Goldstein, A. Kapelner, J. Bleich, and E. Pitkin. 2015. "Peeking Inside the Black Box: Visualizing Statistical Learning with Plots of Individual Conditional Expectation." Journal of Computational and Graphical Statistics 10 (1): 44–65.